HEADLIGHT GLARE SIMULATOR FOR A DRIVING SIMULATOR 2.0

Alex D. Hwang
Schepens Eye Research Institute,
Department of Ophthalmology, Harvard Medical School,
Boston, MA, USA, e-mail: alex.hwang@schepens.harvard.edu

Eli Peli
Schepens Eye Research Institute,
Department of Ophthalmology, Harvard Medical School,
Boston, MA, USA, e-mail: eli.peli@schepens.harvard.edu

ABSTRACT

In this paper, we would like to introduce a second generation of headlight glare simulator to be used with a driving simulator that significantly improves spatial and brightness accuracy of previously developed prototype headlight glare simulator (Fullerton & Peli, 2009). The system combined a programmable off–the-shelf LED display board and a beamsplitter so that the LED lights, representing headlights of oncoming cars, are superimposed over the driving simulator screen. Although the early prototype headlight glare simulator proved the feasibility of the concept, it required precise spatial arrangement of optical components to avoid misalignments of the superimposed images. Due to the spatial limitations of the driving simulator, this ideal set up is hard to achieve in practice and the use of a 2-dimensional beamsplitter plate inevitably introduces parallax. Furthermore, the driver's viewing position varies by driver based on the driver's height and seating position preferences, and this exacerbates the misalignment. In order to minimize the resulting parallax errors, the new glare simulator we report on here has an intuitive calibration procedure (simple drag-and-drop alignment of nine calibration dots on the screen) which defines a set of mapping coefficients for each driver and reduces overall parallax error. In addition to the improvements of spatial synchronization, in order to simulate the dynamics of headlight brightness changes during nighttime driving, a new LED intensity control algorithms based on headlight and LED beam shapes were developed and validated.

Keywords: headlight glare simulator, driving simulator, spatial calibration, optical calibration

INTRODUCTION

Glare can be described as the visual effect of scattering light within the eye caused by a relatively bright light source presented in the visual field (Miller & Benede, 1973; Van den Berg et al., 1986). This light scattering (veiling) reduces retinal contrast across the visual field and thus reduces overall visibility, and causes visual distraction and disturbance (discomfort glare). If

this glare is strong enough, it will induce total black-out (disability glare). This contrast reduction makes it difficult to perform various necessary visual tasks directly related to driving safety, such as detecting pedestrians, detecting on-road objects, following the road lane, and reading traffic signs. In addition, repeated and/or cumulative exposure to glare sources may cause fatigue in nighttime drivers and compromise driving safety. Disability glare as well as discomfort glare caused by oncoming headlights have been highly associated with nighttime traffic accidents (Plainis et al., 2005; Bullough et al., 2008). Pedestrians are much more at risk of collisions in the dark (Sullivan and Flannagan, 2002), and the proportion of drivers involved in such collisions increases with age (Owens and Brooks, 1995).

As the overall population ages, oncoming headlight glare will likely become more of a problem, yet little is currently known about the functional impact or behavioral response to oncoming headlight glare. As the crystalline lens develops age-related opacities (cataract), light scattering increases with consequential glare/veiling effects (De Waard et al., 1992; Sjostrand et al., 1987). Furthermore people with age-related macular degeneration (AMD) have impaired dark adaptation and impaired scotopic sensitivity such that they experience the glare/veiling effect for longer than the actual glare exposure duration and are likely to be more adversely affected by headlight glare (Collins, 1989; Sandberg and Gaudio, 1995). With the increase of both life expectancy and mobility in older age groups, the number of people with cataract and/or AMD who are driving may increase rapidly. Therefore, a greater understanding of the impact of headlight glare could improve road safety for road users of all ages.

Most studies of headlight glare have relied on static glare sources or sources with limited mobility that provides, at best, an oversimplified representation of the real situation (Akashi and Rea, 2001; Shi et al., 2008; Bullough et al., 2002; Flannagan, 1999). The dynamic nature of an oncoming car's headlight glare has not been studied much because of the difficulty of realistic glare simulation. To address that, we developed a prototype headlight glare simulator to be used with a driving simulator (Fullerton & Peli, 2009). The system combined a programmable LED display board and a beamsplitter so that the LED lights are superimposed over the driving simulator's screen. The positions of illuminated LEDs are spatially synchronized with the on screen positions of simulated oncoming traffic's movements, and the light intensities of LEDs are also matched to real world headlight intensities as visible to the driver. Although the early prototype headlight glare simulator proved the feasibility of the concept, and simulated the light levels and the dynamics of the headlight movements to some degree, a few hurdles still remained to be overcome.

The earlier prototype design required precise alignments of its components. The LCD screen of the driving simulator and the LED display board of the glare simulator had to be installed perpendicular to each other, and the beamsplitter has to be positioned at exactly 45 degrees between them. Due to the spatial limitations of the driving simulator, this ideal set-up was hard to achieve and maintain in practice. Furthermore, the relatively short distance between the image merging surface (beamsplitter) and the driver's viewing position inevitably introduces parallax and it makes misalignments more noticeable on the off-center locations. Since the driver's viewing position varies between drivers, due to each driver's height differences and seating position preferences, the magnitude and the direction of misalignments also varies individually, and it prevents the use of static, system-wide, mapping corrections. In order to minimize the

misalignments caused by parallax, we have implemented an intuitive calibration procedure (simple drag-and-drop of onscreen calibration dots) which defines a set of spatial mapping coefficients for each driver. In addition to the improvements of spatial synchronization, in order to simulate the dynamics of headlight brightness changes during nighttime driving, a new LED intensity control algorithms based on headlights and LED beam shapes were introduced and validated.

The improved headlight glare simulator is a valuable tool for testing the impact of headlight glare for drivers of different ages and vision conditions, as well as for evaluating the effect of a variety of vision aids (such as multifocal contact lenses and intraocular lens implants) on nighttime driving.

CONFIGURATION OF THE HEADLIGHT GLARE SIMULATOR

The headlight glare simulator is a combined system of a driving simulator (LE-1500 driver training simulator from the FAAC, Ann Arbor, MI, Figure 1a), a programmable LED display board module (Peggy 2LE programmable LED boards from the Evil Mad Science Laboratory, evilmadscience.com, Figure 1b) and a beamsplitter plate (polycarbonate beamsplitter from the Evaporated Metal Films Corporation, Ithaca, NY, Figure 1c), optically aligned as shown in Figure 1d.

The driving simulator has five 42″ LCD monitors (LG M4212C-BA, native resolution of 1366 × 768 pixels), and they are spatially arranged to span 225° of driver's field of view (horizontally). The central monitor provides 68.2° (horizontal) × 43.5° (vertical) of the scene in front of the vehicle. The driving simulator has a force feedback steering wheel, and a motion seat with three degrees of freedom to induce realistic driving experience. In terms of simulation scenarios, it runs in a 1,600m × 800m virtual world containing urban and rural areas. A scenario development tool box allows us to create precise task-related events for various experimental conditions, including pedestrian movements, autonomous vehicle (traffic) driving paths, and location/timing-based event triggering. During experiments, the driving simulator produces a 30Hz real-time data stream which contains locations and orientations of all scripted objects and the driver's car in the virtual world.

The LED display module has 4 sets of programmable LED boards. Each board has a 25 × 25 array of high intensity LEDs (5mm diameter) installed on a tight grid covering 0.15m × 0.15m. The locations and brightness levels of the LEDs to be lit are controlled through a USB connection. This external glare source (LEDs) is required because conventional LCD screens used in the driving simulator produce less than 200 candelas per square meter (cd/m^2), which is not intense enough to realistically simulate the brightness of real-world headlights. In other words, although a LCD screen can be used to draw the shape of a simulated glare source with white pixels, they do not induce actual glare in the driver's eyes.

The beamsplitter, also commonly known as a "half mirror" or "teleprompter mirror", has optical characteristics of both transparency and reflectancy. The Transparent/Reflect ratio describes how much light incident to the beamsplitter will be reflected, and how much light will pass through it. For example, a 50T/50R beamsplitter reflects 50% of the incident-light and allows 50% of the

incident-light to pass through it. In particular, if a beamsplitter is aligned in 45° between two light sources (LCD screen and LED display), as shown in Figure 1d, simulated driving scenes displayed on the driving simulator screen are visible through the beamsplitter. The LED lights installed on the upper (i.e., "ceiling") surface of the driving simulator produce bright light directed downward. These lights are reflected on the beamsplitter surface. Therefore, a viewer (driver) on the other side sees a superimposed image of the LED lights and the simulated scene. This simple optical configuration gives a freedom of placing an extra light source that does not obstruct the driving simulator display. For the headlight glare simulator described in this paper, a 50T/50R acrylic beamsplitter was used.
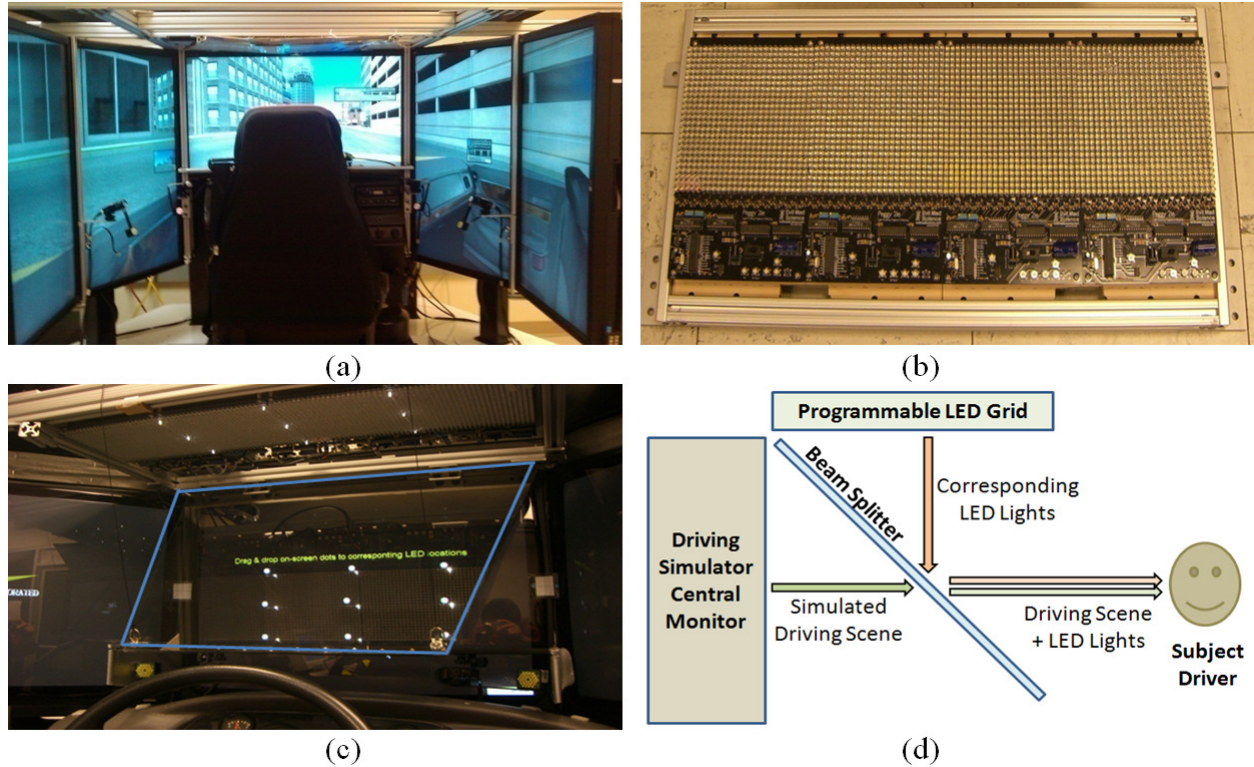

(a)

(b)

(c)

(d)

Figure 1 Components of the headlight glare simulator. (a) FAAC LE-1500 5-LCD screen driver training simulator. (b) Peggy 2 LE programmable LED boards (Note that 4 LED boards were combined to form a 25×100 LED grid). (c) 50T/50R polycarbonate-based beamsplitter plate hanging from the ceiling compartment. A blue outline is added for emphasis. (d) Schematic of the headlight glare simulator in action.

SPATIAL ALIGNMENTS OF TWO LIGHT SOURCES

As briefly described in the previous section, the headlight glare simulator combines lights from two light sources, an LCD screen and an LED grid, facing perpendicularly to each other, using a beamsplitter. Therefore, precise spatial alignment of onscreen headlights and the corresponding off-screen LEDs to be lit is one of the most important aspects of the headlight glare simulator design. In the ideal conditions, where 1) the beamsplitter is aligned at exactly 45° between two light sources, 2) the two light sources are placed an equal distance from the beamsplitter, and 3) a driver is sitting relatively far away from the light sources, perfect alignments will be

automatically accomplished. However, due to the physical space limitation of the driving simulator, this ideal setting is impossible to achieve and introduces parallax. Furthermore, the amount of parallax visible to a driver depends on driver's height and his/her preferable seating position. In order to solve this problem, we have developed a simple calibration process that generates a spatial mapping function between two light source surfaces for each driver. In this section, we will discuss general assumptions about the driving simulator's coordinate system and how this new calibration/mapping procedure can help to convert the oncoming car's headlight positions in the virtual world to the LED grid coordinates in the real world.

Computing Onscreen Headlight Locations in Pixels

The driving simulator renders five directional views of the virtual world onto each corresponding screen based on an assumption that a driver's view point is located at a specific location in the physical world (0.735m away from the center of the central screen and the two peripheral screens). This fixed driver's view point makes rendering and designing of the driving simulator system much simpler because it means that the only dynamic factors that affect onscreen views of the driving scene are limited to the orientation and location of the driver's car and other objects in the virtual world. This, however, can be considered as a limitation of the driving simulator's simulation because the views drawn on LCD screens are not adjusted for changes in the driver's head position in the car. While this results in imperfect simulation, it is generally not a problem.

The driving simulator produces a data stream which contains location and orientation information of all scriptable objects (including traffic such as oncoming cars) as well as location and orientation information of the driver's car based on a virtual world coordination system. The virtual world coordination system is a Cartesian coordination system with respect to a predefined center of the virtual world (see Figure 2a).
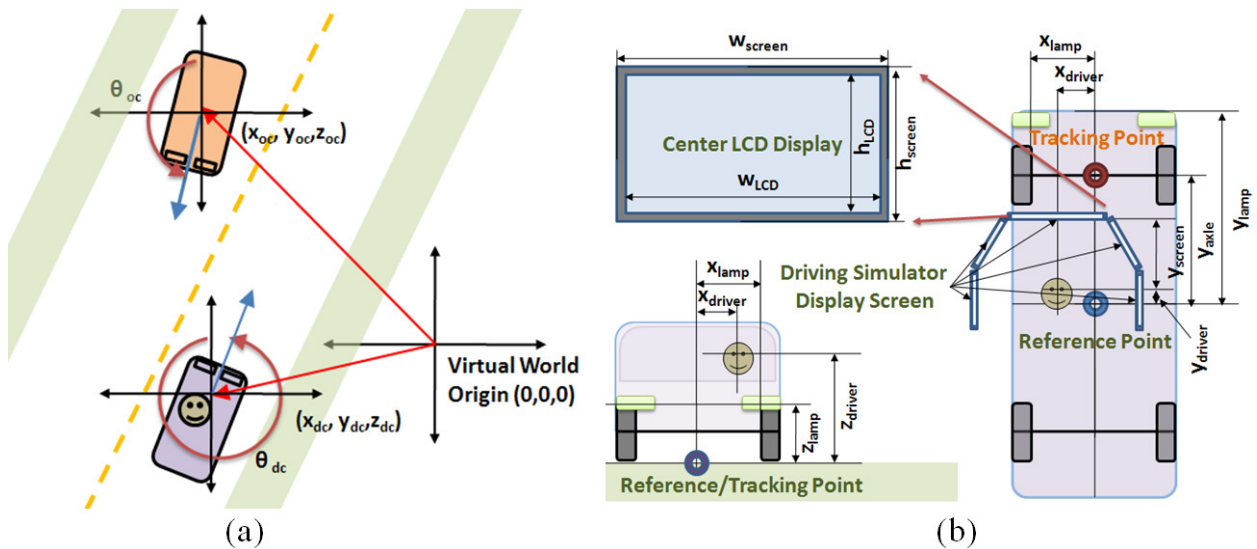

Figure 2 Schematics of a) Driver's car and an oncoming car's locations and orientations measured in the virtual world coordinate system. b) Dimensions of a visual vehicle model.

Note that the position of the scripted object (oncoming car) is based on the car model's reference point (the point between the centers of the front and rear axles), while the driver car's position is tracked by the center of the front axle (see Figure 2b). Therefore, offsets for the headlamp positions and for the driver's viewing position from its reference/tracking point should be carefully considered during the computation.

In order to find the headlamp positions projected on the screen in pixels, we first convert the virtual world coordinates of the oncoming car's headlamp positions to the relative spherical-polar coordinates centered at the driver's head position. Then we compute the projected headlamp positions on a virtually-placed center screen. Finally, these positions in the virtual screen get converted to the pixel coordinates of the real world LCD screen using a mapping function between physical dimensions of the center screen ($W_{LCD} \times H_{LCD}$) and its native resolution (1366 pixels × 768 pixels).

Assuming that the oncoming car (OC)'s location is (x_{oc}, y_{oc}, z_{oc}) and its heading is θ_{oc}, and the driver's car (DC) is located at (x_{dc}, y_{dc}, z_{dc}) and its heading is θ_{dc} in the virtual world coordinate system, as shown in Figure 2a, we can convert the headlight positions (driver side) of an oncoming car using Equations 1-5.

First, we convert the oncoming car's driver-side headlight position to a relative coordinate with respect to the driver's view point, (x_{LH}, y_{LH}, z_{LH}):

$$x_{LH} = x_{oc} + x_{lamp} - (x_{dc} - x_{driver})$$
$$y_{LH} = y_{oc} + y_{lamp} - (y_{dc} - y_{axle} + y_{driver}) \quad\quad (1)$$
$$z_{LH} = z_{oc} + z_{lamp} - (z_{driver})$$

Then, we rotate the coordinate system based on driver's heading direction to get rotated coordinates, (x'_{LH}, y'_{LH}, z'_{LH}):

$$x'_{LH} = x_{LH} \cdot \cos(\theta_{dc}) + x_{LH} \cdot \sin(\theta_{dc})$$
$$y'_{LH} = -y_{LH} \cdot \sin(\theta_{dc}) + y_{LH} \cdot \cos(\theta_{dc}) \quad\quad (2)$$
$$z'_{LH} = z_{LH}$$

Then we convert the Cartesian coordinates to the spherical-polar coordinates based on the driver's view point (d, θ, ϕ):

$$d = \sqrt{x'^2_{LH} + y'^2_{LH} + z'^2_{LH}}$$
$$\theta = \cos^{-1}(\frac{z'_{LH}}{\sqrt{x'^2_{LH} + y'^2_{LH} + z'^2_{LH}}}) \qu\quad (3)$$
$$\phi = \tan^{-1}(\frac{y'_{LH}}{z'_{LH}})$$

where:
d: Euclidean distance to the headlight position
θ: horizontal rotation angle
ϕ: vertical rotation angle

This means that the Euclidean distance to the onscreen contact point is d'$_{screen}$ as defined below. Now, we compute the projection of the headlamp location on the virtual driving simulator screen, (x'$_{os}$, y'$_{os}$, z'$_{os}$). For ease of calculation, the spherical-polar coordinates of the contact point are converted back to Cartesian coordinates using the following equations:

$$d'_{screen} = \frac{y_{screen}}{\cos(\theta) \cdot \sin(\phi)}$$

$$x'_{os} = \frac{y_{screen}}{\tan(\phi)} \cdot \tan(\theta)$$

$$y'_{os} = y_{screen} \cdot \tan(\theta)$$ (4)

$$z'_{os} = \frac{y_{screen}}{\sin(\phi)}$$

Finally, by applying the conversion function as below, we can get the pixel coordinates of the headlamps drawn on center screen, (x$_{os}$, y$_{os}$):

$$x_{os} = \frac{R_H}{2} + \frac{R_H \cdot x'_{os}}{w_{LCD}}$$

$$y_{os} = \frac{R_V}{2} - \frac{R_V \cdot z'_{os}}{h_{LCD}}$$ (5)

where:
R$_H$:   horizontal native resolution of the screen (1366 pixels)
R$_V$:   vertical native resolution of the screen (768 pixels)

Note that the data stream only contains heading (rotation around z-axis) information, and does not contain pitch (rotation around x-axis) or roll (rotation around y-axis) of scriptable objects (oncoming cars). This lack of information, in fact, can be problematic if the driver's car is on a flat road and an oncoming car is on an inclined/declined road because the real headlight positions will be affected by this unspecified self-rotation. On a typical two-lane (4m wide for each lane) with high inclined/declined road (50% grade = 26.57°), when the oncoming car is located at 50m far away from the driver, the projected vertical headlamp displacement due to the object pitch is less than 6 pixels. If the relative pitch value between the driver's car and the oncoming car is kept constant, the amount of displacement on the driving simulator's LCD screen increases as they approach to each other. However, this special case rarely happens on the real-world highway because roads should be designed to avoid "broken back" (frequent change of incline/decline angle) and recommended to have at least 400 feet (120m) of tangent between two incline/decline roads, and transitions should be smooth and continuous. Therefore, large pitch differences between two approaching cars only occur when they are far from each other. If they

are separated enough, this displacement error will be insignificant compared to the angular displacement caused by height differences between two cars.

Mapping Onscreen Pixel Coordinates to LED-Grid Coordinates Using View Calibration

In the previous section we showed how we convert the headlamp positions in the virtual world coordinate system to the relative polar coordinate system of the driver's viewpoint, and how the headlamp position in the spherical-polar coordinate system can be converted to the onscreen pixel coordinates of the driving simulator's central monitor. The glare simulator only covers the central monitor, as glare from cars in the peripheral monitors is generally inconsequential. If we were able to follow the ideal components setup as shown in Figure 1d, mapping between onscreen pixel coordinates to the LED grid coordinate would be a simple linear conversion. Unfortunately, due to the spatial limitations of the driving simulator, we cannot align the components in an ideal way.

In order to superimpose a LED light from the LED grid to a headlight position on the LCD screen, the reflection of LED on the beamsplitter visible to the driver should be located at the headlight location as shown in Figure 3a. If the distances between the LED plane and the beamsplitter plane, and the distance between the beamsplitter plane and the LCD plane are different, linear mapping of a LED reflection will be fall behind or in front of the LCD plane, and this introduces static parallax condition which introduces the alignment error (AE). Since the driver's position is relatively close to the center monitor, AE will be amplified and spread nonlinearly over the simulated driving scene. The AE is minimized at the center of the scene and increases as an incident point to the beamsplitter approaches to the outer border of the screen.

One way to eliminate the AE caused by parallax is developing and implementing a nonlinear mapping function between the LED and the LCD plane. However, this solution is hard to achieve in practice because each driver has different preferable sitting position, and the angle of the beamsplitter should be changed to allow ergonomically comfortable driving space to the driver.
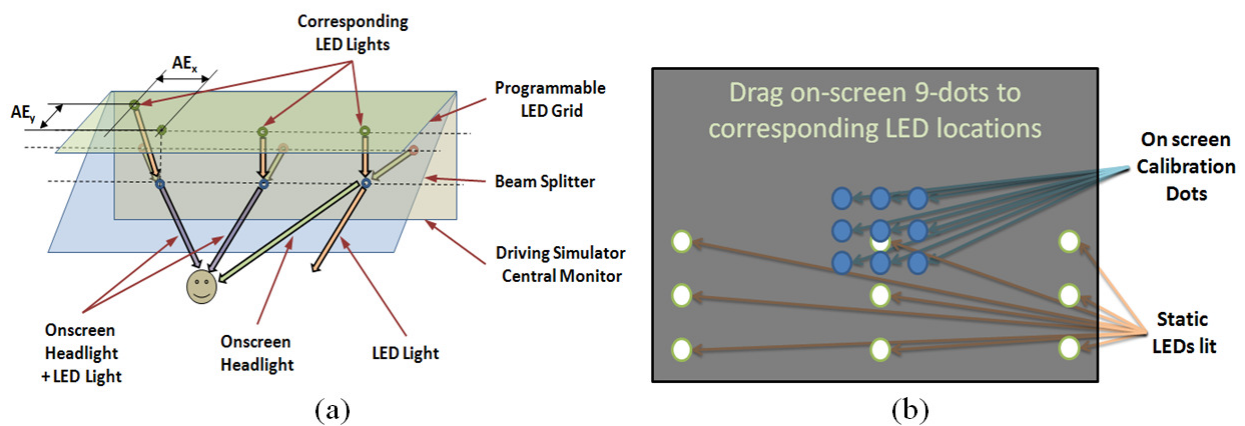

(a)   (b)

Figure 3 Schematics of (a) Alignment error (AE) is larger at eccentric screen positions and minimal at the center, and (b) Initial view of the drag-and-drop calibration process.

Therefore, we decided to resolve this with a simple drag-and-drop type calibration process, which will be performed by each driver before experiments start and will produce a set of spatial mapping coefficients between driving simulator's onscreen surface and LED grid surface. During the calibration process, nine predefined LED positions on the LED grid are lit in low bright level (to reduce the glare) and nine calibration dots appear on driving simulator's central monitor as shown in Figure 3b. Then, the driver is asked to drag each onscreen calibration dot to the corresponding LED light position. Once a driver finishes the task, the coordinates of calibration dots (in pixels) as well as the corresponding LED coordinates are recorded. Since the full LED grid is composed of four 25 × 25 LED grid boards to form a 100 × 25 LED grids, the drivers need to calibrate each LED board to cover the full range of LED grid space. Spatial mapping is based on simple piecewise linear interpolation among calibration dots. The following equation converts onscreen pixel location to corresponding LED grid coordinate, (x_{LED}, y_{LED}):

$$x_{LED} = \left(\frac{x_{os} - x_{os\_L}}{x_{os\_R} - x_{os\_L}} \right) \cdot \left(x_{LED\_R} - x_{LED\_L} \right)$$

$$y_{LED} = \left(\frac{y_{os} - y_{os\_D}}{y_{os\_U} - y_{os\_D}} \right) \cdot \left(y_{LED\_U} - y_{LED\_D} \right)$$

(6)

where:
x_{os}:   horizontal pixel coordinates of a headlight position
x_{os_L}:   horizontal pixel coordinates of a nearest onscreen calibration point on the left
x_{os_R}:   horizontal pixel coordinates of a nearest onscreen calibration point on the right
x_{LED_L}:   horizontal LED coordinates of a corresponding LED on the left
x_{LED_R}:   horizontal LED coordinates of a corresponding LED on the right
y_{os}:   vertical pixel coordinates of a headlight position
y_{os_U}:   vertical pixel coordinates of a nearest onscreen calibration point on the up
y_{os_D}:   vertical pixel coordinates of a nearest onscreen calibration point on the down
y_{LED_U}:   vertical LED coordinates of a corresponding LED above (on the up)
y_{LED_D}:   vertical LED coordinates of a corresponding LED below (on the down)

In summary, since the driving simulator streams out the driver car position and the oncoming car position in virtual world coordinates during the run, we can use Equation 1 through Equation 5 to compute the onscreen headlight positions, and then apply Equation 6 to compute the corresponding LED coordinate. This two steps coordinate mapping processes reduces overall AE for each driver with minimum efforts.

SIMULATION OF REAL WORLD HEADLIGHT BRIGHTNESS

Along with keeping the spatial alignment between the two light sources, another, and possibly more vital part of a successful real world headlight simulation is how well the headlight glare system simulates dynamics of headlight brightness changes during the run. The amount of headlight glare that would be perceived by a driver depends on the amount of projected light from the headlight that finally reaches the driver's eye. Since a typical car uses headlamps designed to produce an anisotropic beam shape (not spherical), in addition to the distance

between a driver's car and an oncoming car, angular distributions of light intensity (beam shape) of a headlight should be considered. In this section, we will briefly describe the current beam shape regulations and related physical characteristics, and then describe how this headlight beam shape and relative cars positions and orientations can be used to compute equivalent LED intensity levels.

Generic Headlight Beam Shape

The U.S. National Highway Traffic Safety Administration (NHTSA) enforces the Society of Automotive Engineers (SAE) standard to reduce glare to oncoming traffics while ensuring enough light is projected forward for safe driving at night (FMVSS, 2007). This regulation defines a set of cutoff values (horizontal and vertical aiming cues that mark low/high limits of projected brightness for headlights) in luminance intensity (candelas, cd), and it sweeps ±15° horizontally and ±5°vertically over a 2-dimensional angular projection surface. For regular low beam headlights, the brightest portion (peak) of the driver side headlamp should be aimed toward the lower-right to reduce the glare that oncoming traffic will see (see Figure 4a). For high beams, headlights should be aimed straight ahead (0°V, 0°H). European countries follow the Economic Commission for Europe (ECE) standards which are conceptually similar to the SAE standards but designed to cause less glare to oncoming traffics. The ECE standards for low beam allow more light toward the upper right to improve readability of road signs (ECE, 2006).

Although these cutoff values define maximum or minimum light intensities for some reference angle points, it is hard to generate a single mathematical model of a 'generic' headlight beam shape because headlight beam shape is a complex 3-dimensional angular function and it is different from headlamp to headlamp. Fortunately, a large survey of headlight beam shapes for the 20 top-selling passenger vehicles in the U.S. and in Europe is available (Schoettle et. al. 2001). In the survey, the luminance intensities at various angular locations were measured, covering ±45°horizontally and -5° to 7° vertically. The angular resolution of measurement points on a projected surface along the horizontal axis was unevenly spaced (0.5° between 0° and 5°, 1° between 5° and 10°, and 5°between 10° and 45°). Luminance intensity measures along the vertical axis were evenly distributed with an angular resolution of 0.5°.

This variable resolution and discontinuity among measured points are tricky for the headlight glare simulator's LED brightness level calculations. In order to create a light distribution that is smooth and continuous, a bilinear interpolation was applied among neighboring data points to bridge the various spatial gaps between data points. Then a 2-dimensional fast Gaussian smoothing (with standard deviation of 0.5°) was applied to the light intensity distribution map to get a smooth headlight beam shape. The resulting distribution map has a uniform angular resolution of 0.5° with a smooth surface. Figure 4a shows the resulting 'generic' headlight beam patterns in U. S. and Europe, measured from the direction against the projection.

Note that the brightness values (gray level) in Figure 4a are normalized to a 0-255 range. Therefore, each plot shows the relative brightness distribution of a given headlight category instead of absolute/real measured values. For example, the peak in the U. S. high beam plot is located at (-0.5°H, 0°V) and its real luminance intensity is 43,604 cd. The peak in the U. S. low beam plot is located at (-3.5°H, -1.5°V) and represents 27,986 cd.
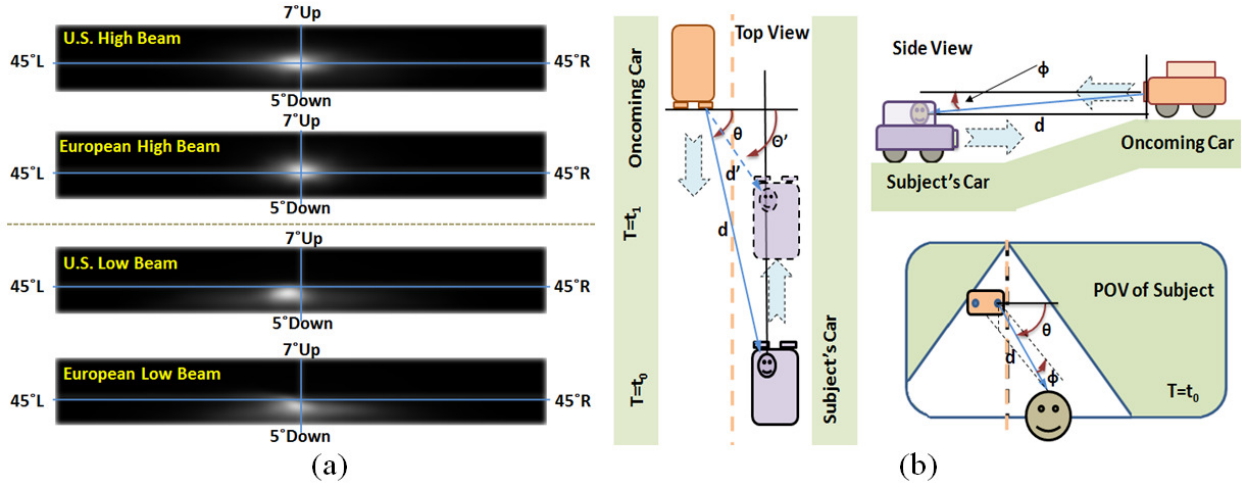
Figure 4 (a) Angular distribution of projected light (beam shape) for high and low headlight beams measured from the front. (b) Schematics of headlight projection angle calculation.

The 75th percentile of measured luminous intensities at each angular positions of the U. S. low beam was used to develop the headlight glare simulator specifications, because it causes more glare. However, the software is designed in a modular way that can accommodate the ECE standard or high beam conditions by simply interchanging the beam shape map.

Dynamics of Luminance Intensity Change

This Angular Light Intensity Distribution Map (ALIDM), in fact, offers a simple way to compute the required brightness intensity level for an LED needed for simulating headlight glare. For example, if a driver's car and an oncoming car are driving towards each other, as shown in Figure 4b, as the distance between two cars (d) decreases, both the horizontal projection angle (θ) and vertical projection angle (ϕ) will increase.

Note that the amount of light reaching the driver is inversely proportional the distance squared (d^2). Since we can convert headlamp locations of oncoming cars to relative spherical-polar coordinates originating at the driver's point of view, we can compute the horizontal projection angles and the vertical projection angles. Moreover, once we know the projection angles, we can locate a corresponding relative brightness level from the angular light intensity distribution map. Finally, the required LED brightness (L_{req}) can be computed with the following equation:

$$\theta_{proj} = \frac{\pi}{2} - \theta$$

$$\phi_{proj} = -1 \cdot \phi \qquad\qquad (7)$$

$$L_{req} = \frac{ALIDM\left[\theta_{proj}, \phi_{proj}\right]}{d^2}$$

11

where:

d: Euclidean distance to the headlight position
θ: horizontal rotation angle
ϕ: vertical rotation angle
θ_{proj}:   horizontal projection angle
ϕ_{proj}:   vertical projection angle

Figure 5 shows plots of horizontal projection angle (Figure 5a) and required LED brightness level (Figure 5b), when two cars are approaching each other from 300m apart on a two-lane road (4m wide). In order to simulate the worst glare case, the vertical projection angle between the two cars is assumed to be -1.5°V (the vertical coordinate of the peak location of the U.S. low beam). This vertical projection angle is assumed to be kept constant during the simulation. As expected, the horizontal projection angle (θ) slowly increases until it reaches around 25m (less than 10° change) then rapidly increases as two cars are approaching more closely (Figure 5a). The required brightness level that needs to be projected to the driver (Figure 5b) shows a similar pattern as the projection angle change, in which the required brightness slowly increases until about 25m. However, the required brightness rapidly drops after about the 7m because of the beam shape of the headlight. The highest required brightness level is around 1,564 cd and it happens when the horizontal projection angle is 29.4°. Considering the brightness level of the peak in the U. S. low beam shape (27,986 cd), this means that actual required brightness that a LED need to produce is about 5.59% of the maximum brightness (peak) of a headlight.
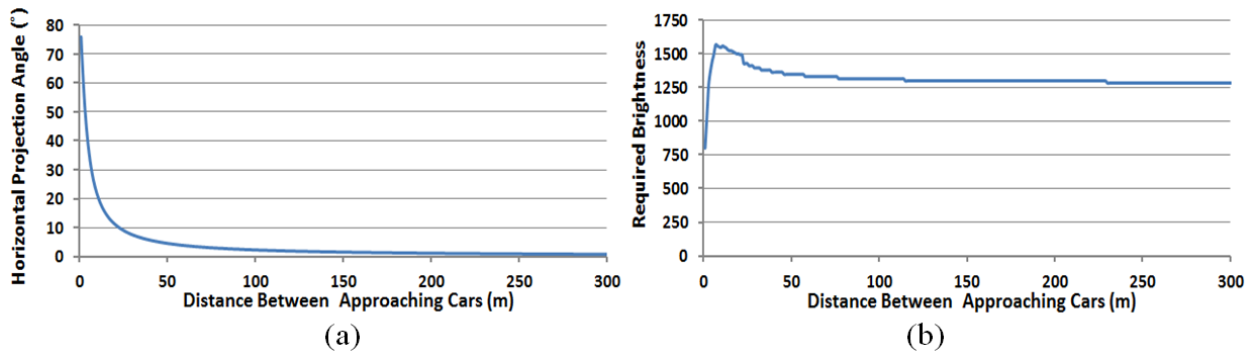

Figure 5 Plots of (a) Horizontal projection angle. (b) Required brightness level. When two cars are approaching each other from 300m on a 2-lane road (lanes are 4m wide)

The assumptions used to generate the plots in Figure 5 do not represent the absolute worst glare case that can possibly happen because the horizontal projection angle does not cross the maximum peak horizontal projection angle (-3.5°H). Although this case can happen when two cars are approaching each other on a curve, it is hard to image that the oncoming car's position is very close to the driver's car (less than 5m) when the peak of the headlight beam shape points right at the driver. This is because of the safe distance between the two cars and the lower-pointed headlight beam direction. Note that even with a very close call of a frontal crash, (assuming that the side gap between two cars is 0.5m instead of 4m) the peak of the required light intensity is 1,575 cd, which is almost the same as the required brightness level. This is possible because the maximum required brightness level occurs when the oncoming car is at 29.05° from the direction of the driver's car and it is about 9m away from the driver.

Programmable LED Board and Quantization.

The early prototype of the glare simulator used an off the shelf programmable LED display board with sparsely populated LEDs (low spatial resolution). Consequently, when smooth headlight movements on the driving simulator screen (high spatial resolution) were simulated by the selection of the LED light on the board, the simulated headlamps appeared to move discontinuously due to large spatial gaps between LEDs on the board. In order to reduce these jumping movements, we have developed customized LED boards which are about 1/4 the size of the original board while holding the same number of LEDs in a 25 × 25 square grid. These new LED boards allow smoother headlight motion simulation. However, due to the reduced size and dense packing of the LED grid, it inevitably requires 4 sets of the LED boards to be deployed simultaneously to cover a wider surface area.

Each LED board contains an ATmega328P microcontroller, two STP16DP05 LED driver chips and a USB/Serial interface to a PC. The boards are controlled by the Arduino compatible Pegy2Serial library. For real-time communication to the board, the Java RXTX serial/parallel communication library is used. The brightness level of individual LEDs depends on the number of positive current pulses supplied to the LED in a given period of time. For example, if there are 375 cycles of current pulses available in a second, but no current is supplied to the LED during the entire time, the perceived brightness will be the darkest (turned off). If the current is always supplied during the entire time, the perceived brightness will be brightest (turned on). If every other current pulse is supplied to the LED, the LED brightness will be half of its maximum brightness. It is possible to produce as many brightness levels as we want with the method described above, but due to the hardware limitations of interrupt frequency and the relatively fast frame rate (at least 60fps) required for LED animations, the number of brightness levels available for the current implementation of the programmable LED board is limited to 16 levels. This means that the required brightness level passed from the previous calculations needs to be quantized into 16 levels. Although it depends on luminance difference between successive steps and on duration of each step, simulation of perceptually continuous brightness change using discontinuous stepping (quantized) brightness levels is certainly possible (Vicario and Zambianchi, 1999). Since the range of the brightness change during the simulation is relatively small as seen in Figure 5b, and quantization is done in relatively fine levels, the luminance difference between each successive step is less than 6%. Therefore brightness level quantization does not induce discontinuous brightness changes.

Measuring LED Beam Shape and Mapping of the Brightness Level

The last but not least among various considerations of simulating real-world headlight brightness is the actual production of the correct amount of light with a high intensity LED. Beside the limited number of brightness levels posed by the hardware, we have to consider the beam shape of the LED itself, similar to the headlight beam shapes, because the positioning of LEDs affects the actual amount of light reaching the driver's eye. The LEDs that we used are the NSPW500DS white LED from Nichia (Tokushiba, Japan) and the manufacturer provided basic electrical/ optical specifications for it. However, the information provided is not detailed enough to build as complete an angular distribution model of the LED beam shape as we generated for

the headlights. It is still possible to follow a similar measurement procedure that used to build a headlight beam shape, as described in the headlight beam shape survey (Schoettle et. al. 2001), to build an angular distribution of LED light intensity, but we used a simpler and more robust method to capture the LED beam shape using a digital camera.

To achieve the goal, an LED was lit at its maximum brightness and the LED board that was placed on a flat surface so that the LED light was aiming directly upward. A glass plate was installed 0.1m away from the LED, and a digital camera was set 0.5m away from the LED. The camera was set to aim straight down at the LED with no automated mode turned on. We placed a sheet of rectangular grid paper on the glass plate and manually adjusted the camera focus to get a sharp image of the grid. After taking a picture of the spatial grid, the grid paper was replaced by a neutral density (ND) filter and we took a picture of the projected beam shape on the ND filter with ambient light turned off. The optical density of the filters applied was increased until pixel saturation (whiteout portion of the picture) disappeared. Since all of the pictures were taken at the same location, the same spatial coordinates apply to each picture that captures the spatial distributions of the light.

A pixel substitution algorithm was applied for integration of the images taken. First, the algorithm searched for saturated pixels from the non-ND filtered image, and then replaced those pixels with 'spatially' corresponding pixels from the next level ND filtered image. When a saturated pixel is substituted, the white level of the pixel needs to be adjusted to compensate for the light reduction done by the ND filter. For example, if a saturated pixel (pixel value of 255 in an 8-bit grayscale image) in a non-filtered image is replaced by a corresponding pixel in the next level ND filtered image, if the filter applied was a 10% light reduction ND filter, we apply the following conversion function to recover the original pixel value.

$$v_{rescued}{'} = v + \frac{v}{(100-r)} \cdot r \qquad (8)$$

where:
$v_{rescued}$: corresponding pixel value rescued from the ND filtering
v: corresponding pixel value of the next level ND filtered image
r: percent reduction transmittance of the ND filter

After processing of each ND filtered image, the pixel values need to be normalized to 0 to 255 ranges before continuing the pixel substitution process for the next level. Finally, the Gaussian smoothing of SD=0.5° is applied to produce a final angular light distribution map for the LED as shown in Figure 6a. The angular coordinates of pixel locations were computed from the picture of the rectangular grid. This wide dynamic range photography enabled us to measure the dynamic range of the LED, which is much higher than that of a single camera.

The circular beam shape of the LED indicates that LEDs located further from the center of the screen need to produce more light than the ones located near the center of the screen to provide the same required brightness level.
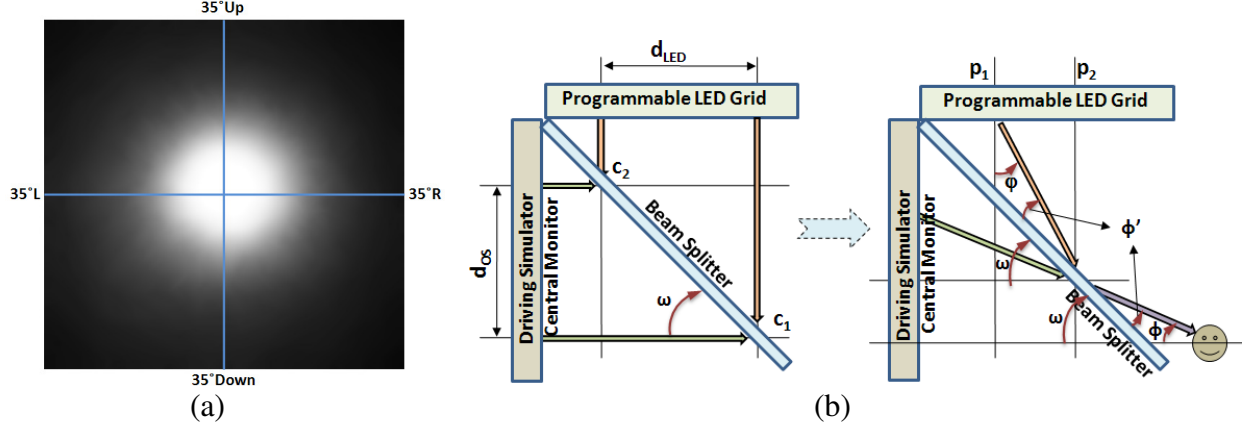
14

Figure 6 (a) A plot of angular light distribution of a LED. Note that LED beam shape is circular. (b) Schematic of the light projection angle calculation for the LED.

Since we already have a mapping function between the onscreen positions and the LED grid coordinates, as well as physical size of a pixel on the LCD screen (0.000681m), and single LED grid width (0.006m) of the LED boards, we can compute the beamsplitter angle (ω) by computing the arctangent of the ratio between the physical distance of two onscreen calibration positions along the vertical center line and distance between corresponding LED locations (see Figure 6a left).

$$\omega = \arctan(\frac{d_{os}}{d_{LED}}) = \arctan(\frac{h_{LCD} \cdot (y_{LCD\_U} - y_{LCD\_L})}{h_{LED} \cdot (y_{LED\_U} - y_{LED\_L})}) \qquad (9)$$

where:

h_{LCD}:   height of a pixel on the LCD screen (0.000681m)
h_{LED}:   height of a LED on the LED grid (0.006m)
y_{LCD_U}:   vertical coordinate of upper calibration dot position
y_{LCD_L}:   vertical coordinate of lower calibration dot position
y_{LED_U}:   vertical coordinate of corresponding upper calibration LED position
y_{LED_L}:   vertical coordinate of corresponding lower calibration LED position

Once we know the beamsplitter angle, we can compute the LED projection angle (φ) using Equation 10, and decide the LED brightness level in a manner similar to the one used for the headlight beam shape computation.

$$\phi' = 180 - (180 - \omega) - \phi$$
$$\varphi = 180 - (\omega + \phi') = 180 - 2 \cdot \omega + \phi \qquad (10)$$

where:

ϕ: vertical component of the driver's viewing angle.

It is also necessary to take into account that the beamsplitter used has an optical characteristic of 50R/50T which means that only 50% of the light produced by the LED is delivered to the driver's eye. Therefore, the final brightness level of the LED should be twice the required LED brightness modulated by the angular brightness distribution map of the LED discussed above.

Simulation Performance of Real-World Headlight

All of the brightness computation is based on the relative brightness value assuming that the peak brightness of the 'generic' headlight and the peak brightness of the LED are compatible. This means that the LED used is able to produce enough light to simulate the amount of light produced by the oncoming traffic's headlight reaching the driver's eye at the worst case. In order to check the simulation compatibility, the peak luminance for LEDs and headlights were measured using Minolta LS-100 luminometer. The peak luminances of 5 LEDs were measured from 1.0m away at (0°V, 0°H) and the value was $47,221 \pm 2,424$ Cd/m^2. For the real world headlight, the peak luminances from three cars were measured at 2.0m away and it was $104,051 \pm 15,283$ Cd/m^2. This means that if they are measured at the same distance, the amount of the light reaching the driver from a LED is only about 11.36% of the amount of light from a headlight. Furthermore, if we consider the luminance reduction due to the beamsplitter, the ratio is reduced to 5.78%. However, in the simulation results for the presumed worst case, (as shown in Figure 5b), the worst glare condition happens at 7m from the driver's view position and it requires about 5.59% of the peak headlight brightness. Therefore, we can safely conclude that for simulation of headlight brightness the brightness of our LED is sufficient, and the brightness mapping using headlight and LED beam shapes is valid. Figure 7a-f shows the headlight glare simulator in action using a photograph of the screen/beamsplitter combination.

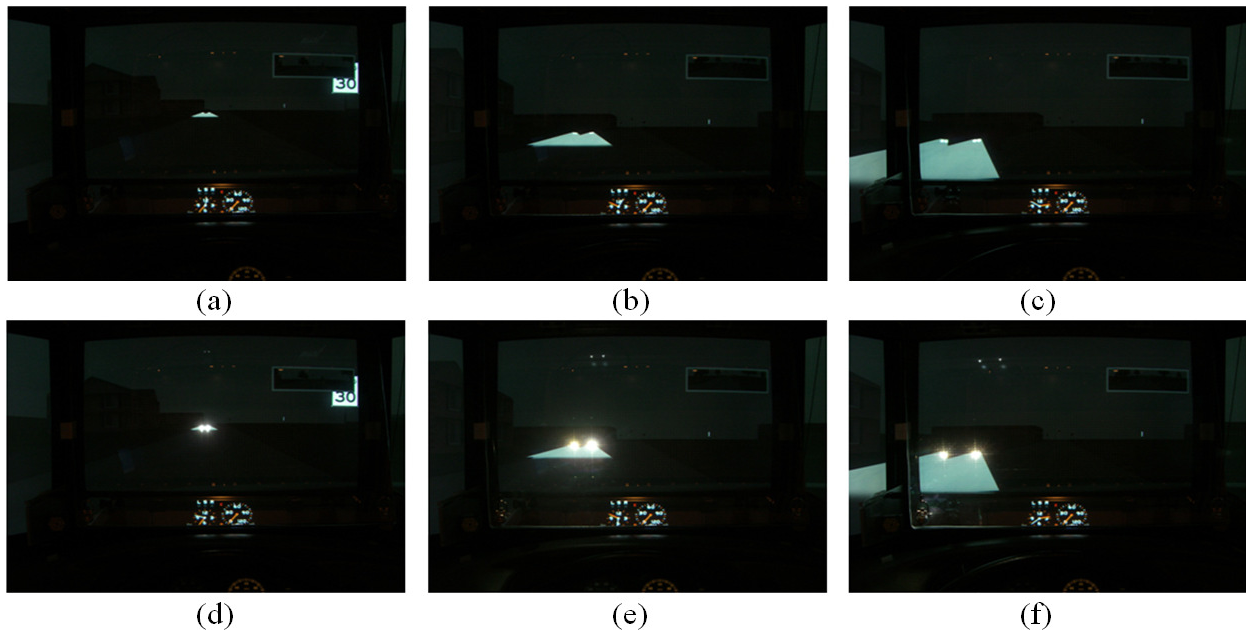|		
(a)	(b)	(c)
(d)	(e)	(f)

Figure 7 Simulation of night driving on a driving simulator. (a)-(c) Without the headlight glare simulator. (d)-(e) With the headlight glare simulator turned on. The 3 simulations represent 3 distances between the cars.

SIMULATION OF REAL WORLD HEADLIGHT SIZE

Another dynamic factor which might be important for simulating the real-world headlight is the dynamic changes of the glare source angular size. The driver's perception of the visible size of the glare source (headlamp) increases as the oncoming car approaches the driver's car. For example, if an oncoming car approaches and reaches about 7m away from the driver's car, a regular-sized headlight (0.1m×0.3m) covers about 0.82°×2.45° of driver's visual angle. Simulation of the gradual size change requires a much finer spatial resolution LED grid than the current LED board of choice provides (currently, each LED covers 0.45° in visual angle). For the case of larger expansion of headlight size (when an oncoming car is close to the driver's car), we considered using multiple adjacent LEDs to be lit while keeping the total amount of light from individual LEDs to the driver's eye to be the same as the required light amount. However, because of the relatively coarse spatial resolution of the LED board, the multiple LEDs lit look like multiple glare sources instead of the single glare source we perceive for individual headlight. Fortunately, a previous headlight glare study using static real world glare sources, done by Bullough et al. (2003), reported that the size of glare source does not affect the peripheral detection performance of the driver. Therefore, we made a design decision to use a single LED to simulate a single headlight regardless of its size variation.

CONCLUSIONS

This paper has described a novel development of a headlight glare simulator using a set of programmable LED grid boards and a beamsplitter plate that can be installed on an existing driving simulator. The LEDs on the board produce brighter lights that conventional LCD displays cannot produce. The beamsplitter installed between the LCD screen and LED board superimposes the lights from the LEDs to the virtual world rendered on the LCD screen. The successful simulation depends on how well a glare simulator can synchronize the spatial movements of the oncoming headlight positions with LED movements, and how well a simulator mimics the corresponding real-world headlight brightness which varies based on spatial positioning of a driver's car and oncoming traffic.

For spatial synchronization, we have employed a simple intuitive calibration method to get a spatial mapping function between virtual world coordinates and the LED grid coordinates. During an actual drive in the driving simulator, the system computes the coordinates of LEDs to be lit using the calibration mapping function based on a real time data stream from the driving simulator. For accurate LED brightness simulation, the real-world beam shapes of the 'generic' headlight as well as the beam shape of the LED were considered when computing the corresponding LED light level. The range of headlight brightness required for the simulation of the worst glare case has been analyzed to ensure the validity of the headlight simulation.

The system still needs to be validated further through various behavioral comparison studies. In such studies, normally sighted subjects will perform a detection task while driving a real car and being exposed to the real world headlights in a controlled course. A subject will need to react to each appearance of target objects using the horn. Then the same drivers will perform the same task under comparable conditions in a driving simulator with the headlight glare simulator. By

comparing the detection performance (detection rate and reaction time) between those two experimental conditions, we can further increase our confidence in the validity of the headlight glare system.

With the safe and repeatable nature of driving simulator studies, and the development of a realistic headlight glare simulator such as the one shown here, we open new opportunities to study the real-world effects of headlight glare during nighttime driving conditions. For example, this can be used to evaluate the nighttime driving of older people with and without vision impairments and to address the safety issues of ophthalmic devices (e.g., multifocal intraocular lenses) to determine if they impair or aid nighttime driving. The results of those studies will provide evidence to impact future decision-making in determining nighttime driving privileges and restrictions imposed on people with vision impairment (Peli and Peli, 2002).

ACKNOWLEDGEMENTS

REFERENCES

Akashi, Y. and Rea, M. (2001). "The effects of oncoming headlight glare on peripheral detection under a mesopic light level". *Proceedings of the Progress in Automobile Lighting Symposium*, Darmstadt Germany, Darmstadt University of Technology; 2001, 9-22.

Bullough, J. D., Van Derlofske, J., Dee, P., Chen, J. and Akashi, Y. (2003). "An Investigation of Headlamp Glare: Intensity, Spectrum and Size". DOT#80, Washington: U. S. Department of Transportation, National Highway and Traffic Safety Administration.

Bullough, J. D., Fu, Z. and Van Derlofske, J. (2002). "Discomfort and Disability Glare from Halogen and HID Headlamp Systems". *Advanced Lighting Technology for Vehicles, SAE SP-1668.* Paper # 2002-01-0010, 2002.

Bullough, J. D., Skinner, N. P., Pysar, R. M., Radetsky, L. C., Smith, A. M., and Rea, M. S. (2008). "Nighttime glare and driving performance: Research findings". *DOT# HS-811-043*, Washington: U. S. Department of Transportation, National Highway and Traffic Safety Administration.

Collins M. (1989). "The onset of prolonged glare recovery with age". *Ophthalmic Physiology Optics*, 9:368-71.

Sandberg M. A. and Gaudio A. R. (1995). "Slow photostress recovery and disease severity in age-related macular degeneration". *Retina*, 15:407-12

De Waard, P. W., Jspeert, J. K., Van de Berg, T. J. and De Jong P. T. (1992). "Intraocular light scattering in age-related cataracts*". Invest. Ophthalmol. Visual Sci.,* 33(3):618-625.

Economic Commission for Europe (ECE) (2006). "ECE 112: Uniform provisions concerning the approval of motor vehicle headlamps emitting an asymmetrical passing mean or driving beam or both and equipped with filament lamps". *Regulation § 112*, 2006

Federal Motor Vehicle Safety Standard (FMVSS). (2007). "Federal Motor Vehicle Safety Standard #108: Lamps, reflective devices, and associated equipment". *Code of Federal Regulations*, Office of the Federal Register, DC, Washington, § 571.108.

Flannagan, M. J. (1999). "Subjective and Objective Aspects of Headlamp Glare: Effects of Size and Spectral Power Distribution". *University of Michigan Transportation Research Institute UMTRI-99-36*. Ann Arbor, MI: The University of Michigan Transportation Research Institute

Fullerton M. and Peli E. (2009) "Development of a system to study the impact of headlight glare in a driving simulator". *Proceedings of the 5th International Driving Symposium on Human Factors in Driver Assessment, Training and Vehicle Design*, Montana, USA. June 22-25, pp.412-418.

Miller, D. and Benedek, G. (1973). *"Intraocular light scattering: Theory and clinical application"*. Charles C. Thomas, Springfield, Illinois

Owens D. A. and Brooks J. C. (1995). "Drivers' Vision, Age, and Gender as Factors in Twilight Road Fatalities". *University of Michigan Transportation Research Institute UMTRI-95-44*. Ann Arbor, MI: The University of Michigan Transportation Research Institute.

Peli, E. and Peli, D. (2002). "*Driving with Confidence: A Practical Guide to Driving With Low Vision*". P.192, Singapore: World Scientific.

Plainis, S., Murray, I. J., and Charman, W. N. (2005). "The role of retinal adaptation in night driving". *Optom Vis Sci*, 82, 682-688.

Sandberg, M. A. and Gaudio, A. R. (1995). "Slow photostress recovery and disease severity in age-related macular degeneration". *Retina.* 1995; 15(5):407-12.

Schoettle, B., Sivak, M. and Flannagan, M. J. (2001). "High-beam and low-beam headlight patternsin the US and Europe at the turn of the millennium". *University of Michigan Transportation Research Institute UMTRI-2001-19*, Ann Arbor, MI: University of Michigan Transportation Research Institute.

Shi, W., Lockhart, T. E. and Arbab, M. (2008)."Tinted windshield and its effects on aging drivers' visual acuity and glare response". *Safety Science*, 46, 1223-1233.

Sjostrand, J., Abrahamsson, M., and Hard, A. L. (1987). "Glare disability as a cause of deterioration of vision in cataract patients". *Acta Ophthalmol Suppl*, 182, 103-106.

South Dakota Department of Transportation (2011). "Road Design Manual: Chapter 6-Vertical Alignment". *SDDOT Chapter 6*, USA. June 22-25, 2009. pp.412-418.

Sullivan, J. M. and Flannagan, M. J. (2002). "The role of ambient light level in fatal crashes: inferences from daylight saving time transitions". *Accident Analysis and Prevention*, 34:487-498.

Vicario, G. B. and Zambianchi, E., (1999), "On continuity perception in brightness change". Perception, 28 ECVP Abstract Supplements.

Van den Berg, T. J., Van Rijn, L. J., Kaper-Bongers, R., Vonhoff, D. J., Volker-Dieben, H. J., Grabner, G., Nischler, C., Emesz, M., Wilhelm, H., Gamer, D., Schuster, A., Franssen, L., de Wit, G.C., and Coppens, J.E. (2009). "Disability glare in the aging eye: Assessment and impact on driving". *Journal of Optometry*, 2, 112-118.